

Supplementary Information

Mechanistic basis for maintenance of CHG DNA methylation in plants

Jian Fang^{1,4}, Jianjun Jiang^{2,3,4}, Sarah M. Leichter^{2,3,4}, Jie Liu³, Mahamaya Biswal¹, Nelli Khudaverdyan¹, Xuehua Zhong^{2,3,*}, Jikui Song^{1,*}

¹Department of Biochemistry, University of California, Riverside, CA 92521, USA

²Laboratory of Genetics, University of Wisconsin-Madison, Madison, WI 53706, USA

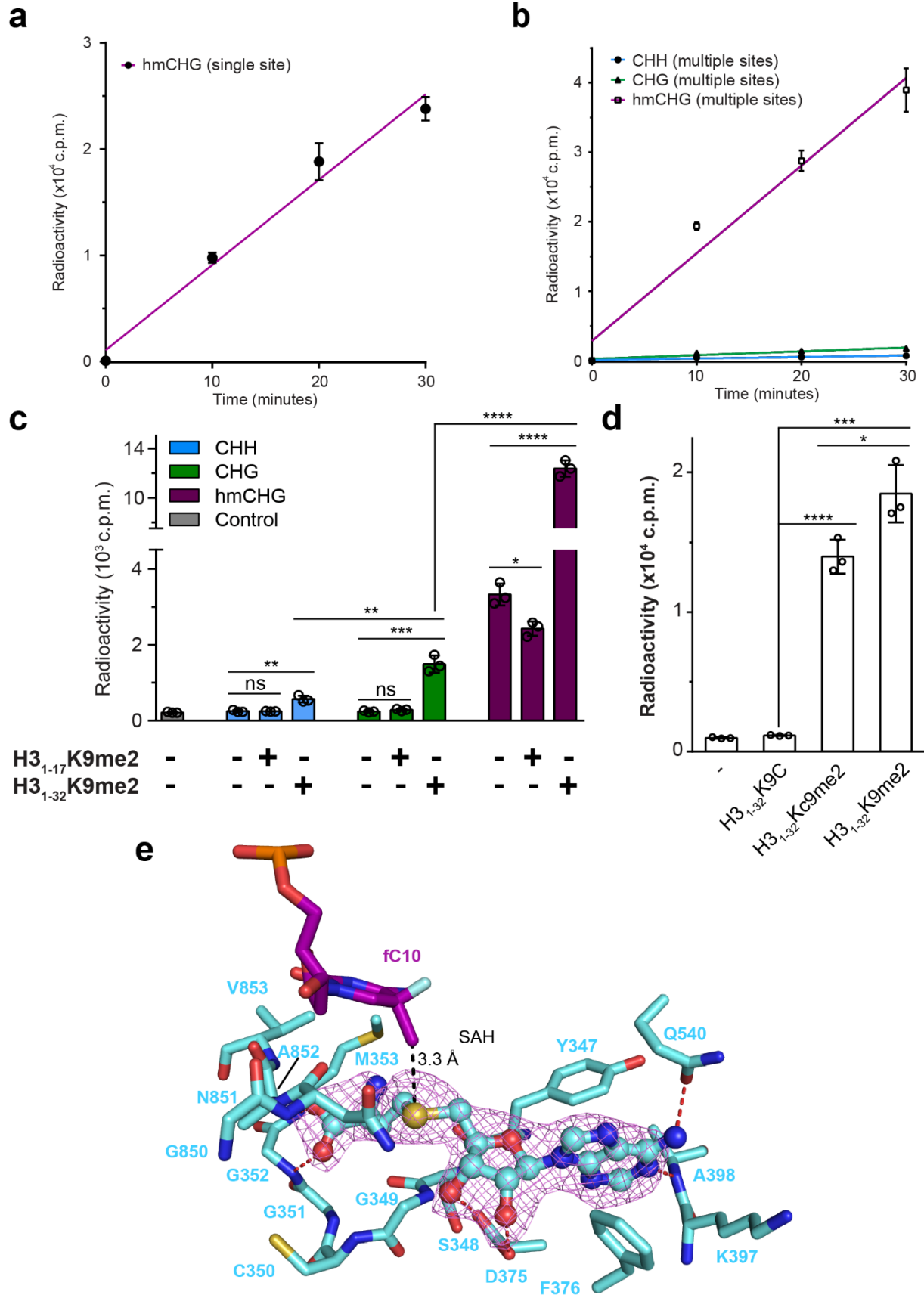
³Wisconsin Institute for Discovery, University of Wisconsin-Madison, Madison, WI 53715, USA.

⁴These authors contributed equally to this work

*Correspondence: xuehua.zhong@wisc.edu or jikui.song@ucr.edu

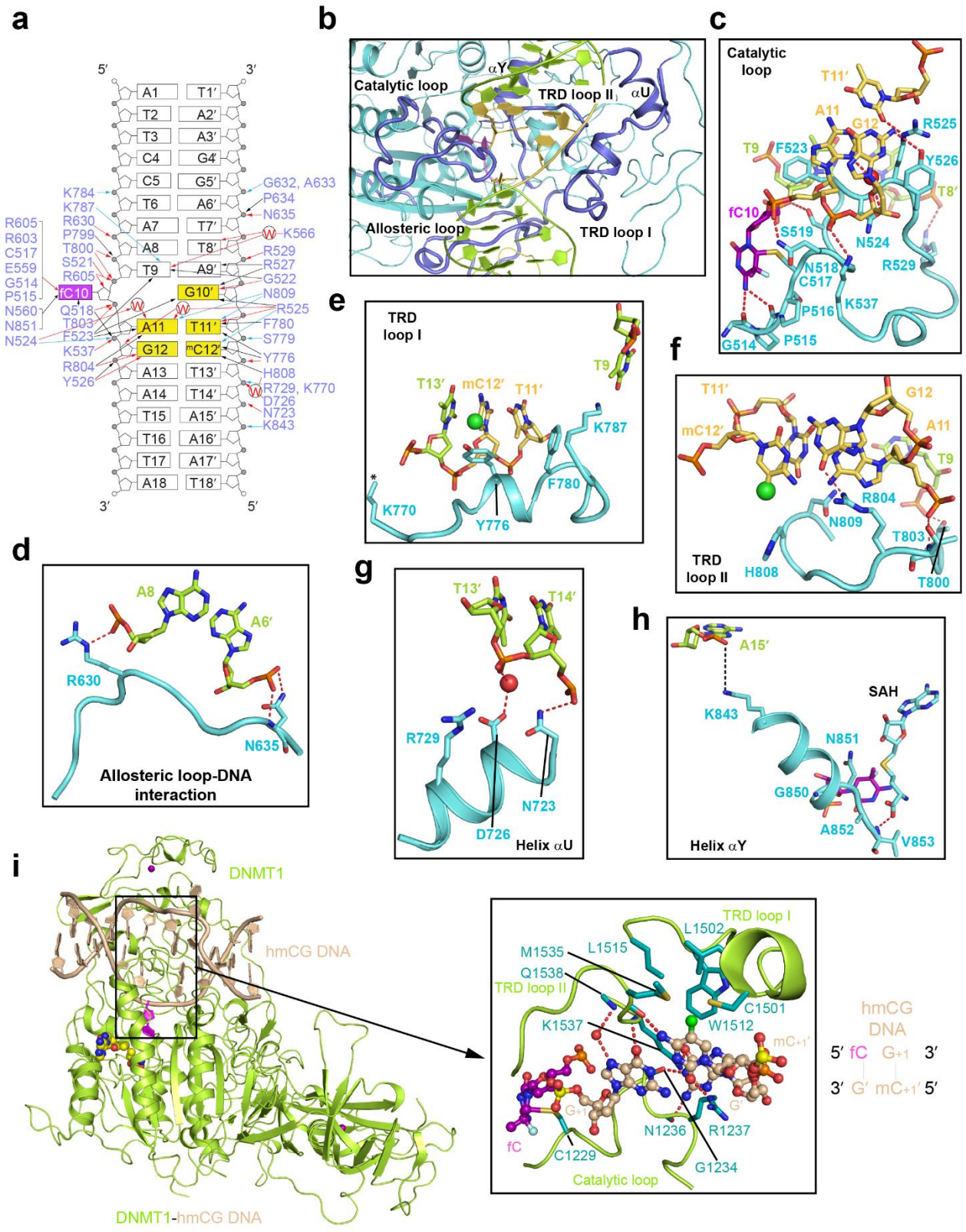
Supplementary Fig. 1 | Sequence analysis of CMT3 proteins from various species.

(a) Domain architecture of ZMET2 and *Arabidopsis* CMT3, with individual domains color-coded and delimited by residue numbers. (b) Sequence alignment of ZMET2 with CMT3 proteins from various plant species. Strictly conserved residues are colored white in red background. Partially conserved residues are colored red. The DNA-, H3K9me2 peptide-, and SAH-binding sites are indicated by red, black and blue asterisks, respectively, on top. Individual domains and enzymatic motifs are also labeled on top.



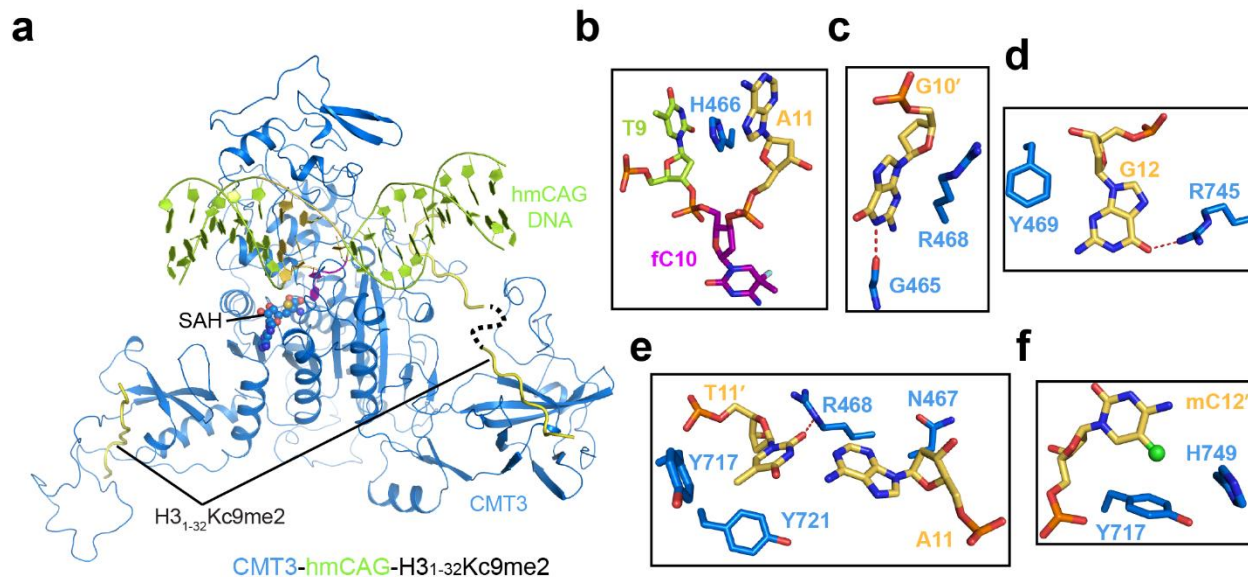
Supplementary Fig. 2 | Enzymatic and structural analysis of CMTs.

(a,b) *In vitro* enzymatic assays of ZMET2 on DNA containing single hmCHG site (a) or multiple CHH, CHG or hmCHG sites (b). (c) *In vitro* DNA methylation assay of CMT3 on DNA duplex containing multiple CHH, CHG, or hmCHG sites, in the presence or absence of H3K9me2 peptides. Control, no substrate present. Data are mean \pm s.d. (n = 3 biological replicates). Statistical analysis used two-tailed Student's t-test. No adjustments were made for multiple comparisons. ns, not significant; *, $p < 0.05$; **, $p < 0.01$; ***, $p < 0.001$; ****, $p < 0.0001$. (d) *In vitro* DNA methylation assays of ZMET2 on DNA containing single hmCHG target site in the presence or absence of K9C-mutated H3₁₋₃₂, H3₁₋₃₂Kc9me2 or H3₁₋₃₂K9me2 peptide. Data are mean \pm s.d. (n = 3 biological replicates). Statistical analysis used two-tailed Student's t-test. No adjustments were made for multiple comparisons. ns, not significant; *, $p < 0.05$; ***, $p < 0.001$; ****, $p < 0.0001$. (e) Close-up view of the SAH-binding site of ZMET2, with the Fo-Fc omit map (violet) for the SAH molecule contoured at 2.0σ level. The distance between the 5-methyl group of fC10 and sulfur atom of the SAH molecule is marked. Source data are provided as a Source Data file.



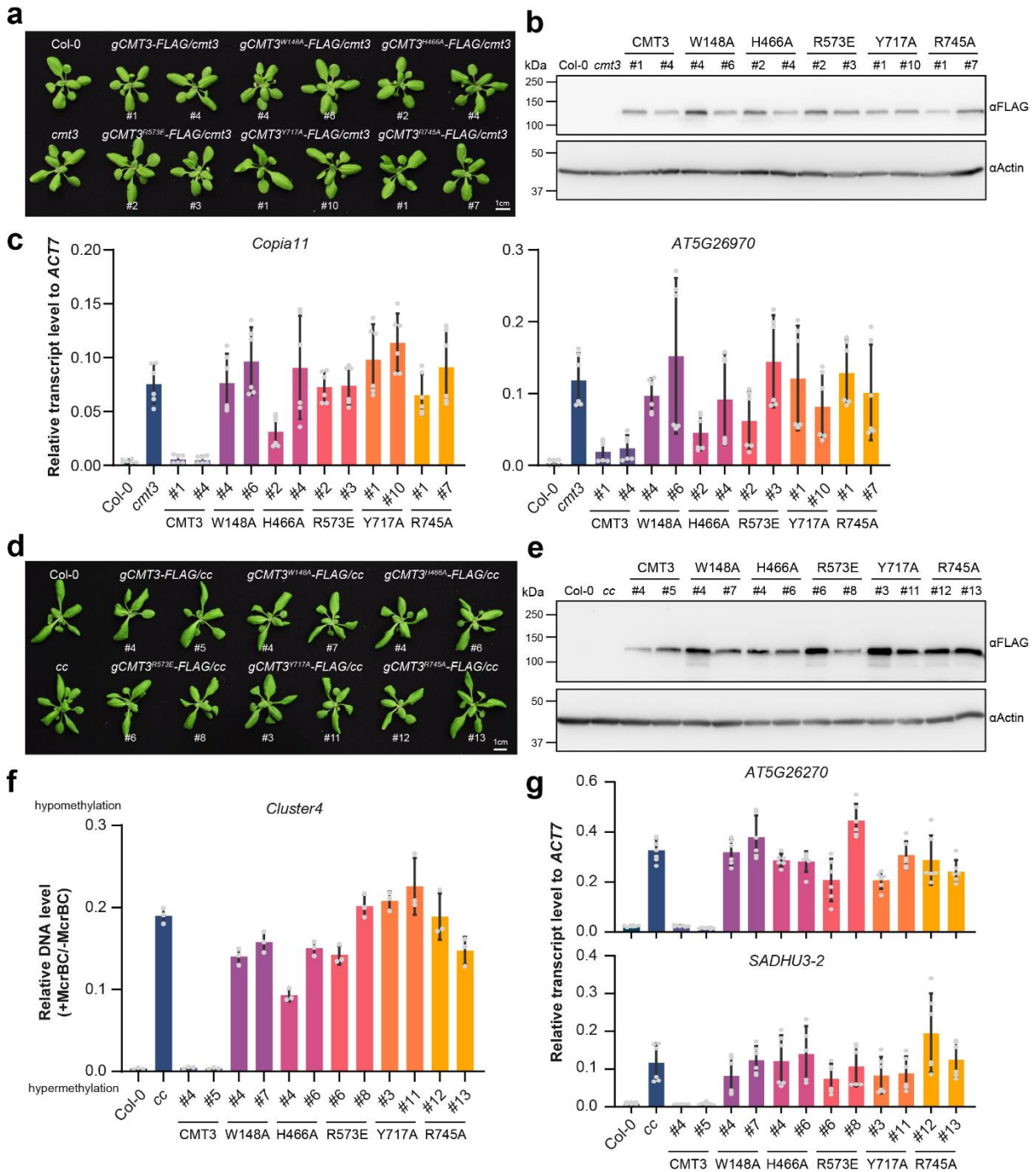
Supplementary Fig. 3 | Structural details for the ZMET2-hmCAG interaction.

(a) Schematic view of the ZMET2-hmCAG interactions. Hydrogen-bonding, electrostatic, and van der Waals contacts are indicated by red, cyan, and black arrows, respectively. Water-mediated hydrogen bonds are labeled by letter 'W'. (b) Structural overview of the structural elements of ZMET2 responsible for DNA binding, colored in slate. (c-h) Close-up view of the DNA interaction by the catalytic loop (c), allosteric loop (d), TRD loop I (e), TRD loop II (f), Helix α U (g) and Helix α Y (h). The hydrogen-bonding and van der Waals contacts are depicted as red and black dashed lines, respectively. The water molecule is shown as red sphere. (i) Ribbon diagram of mouse DNMT1 (limon) in complex with hemimethylated CG DNA (wheat) (PDB 4DA4), with the interactions for base-specific recognition of the fCG/mCG motif shown in expanded view. The hydrogen bonds are shown as dashed lines. The DNA-interacting residues of DNMT1 is labeled. The 5-methyl group of 5mC on the target strand is shown as a green sphere.



Supplementary Fig. 4 | Structural model of the CMT3-hmCAG-H3Kc9me2 complex.

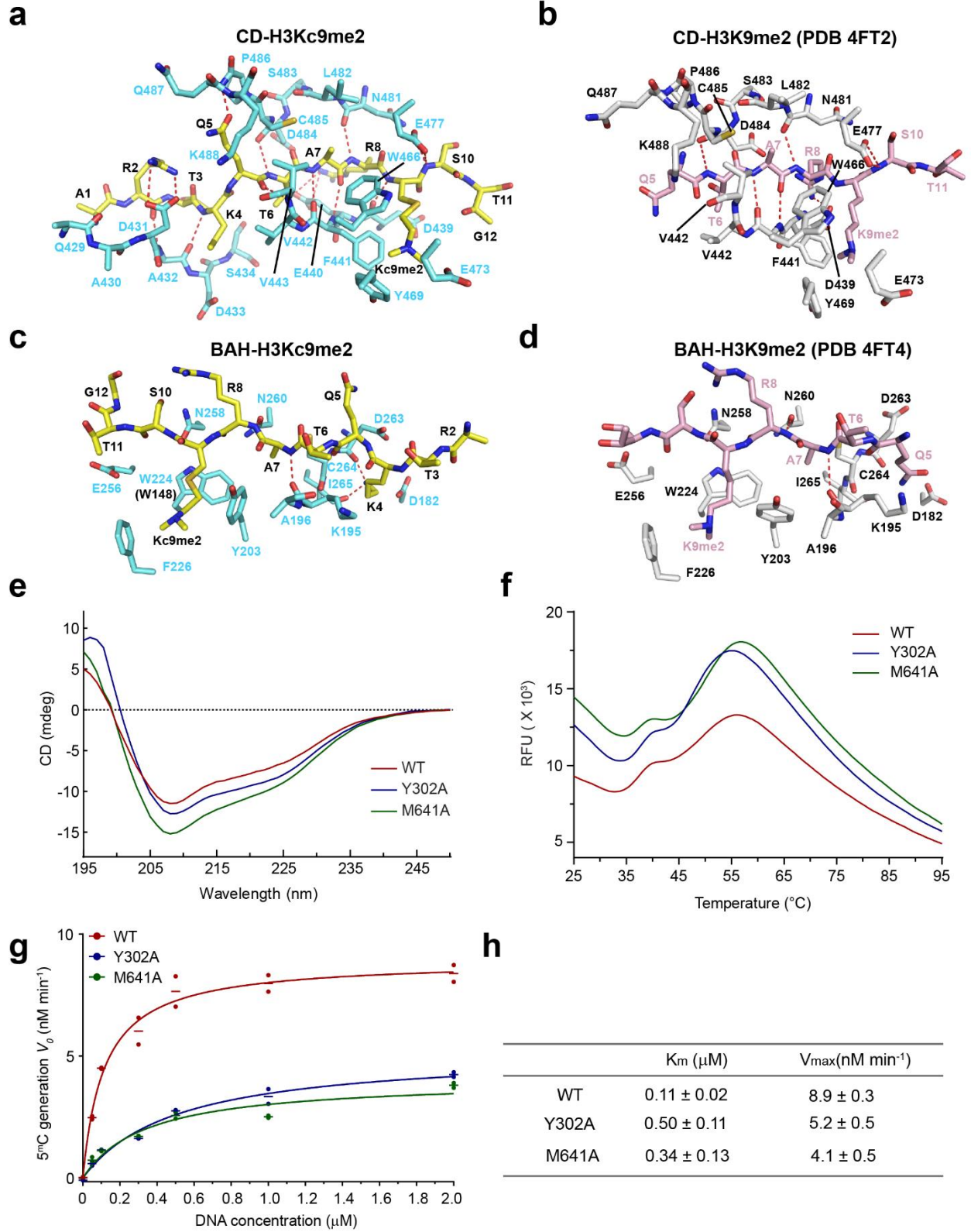
(a) Structural overview of the CMT3-hmCAG-H3₁₋₃₂Kc9me2 complex. The disordered residues T11-G13 of the H3₁₋₃₂Kc9me2 peptide is shown as a dashed line. (b-f) Close-up view of the CMT3-DNA interactions at the DNA cavity after fC10 flipping (b), orphan G10' site (c), CHG guanine G12 (d), +1-flanking A11-T11' pair (e), and mC12' (f). The hydrogen bonds are shown as dashed lines.



Supplementary Fig. 5 | Effect of CMT3 mutations on genomic DNA methylation.

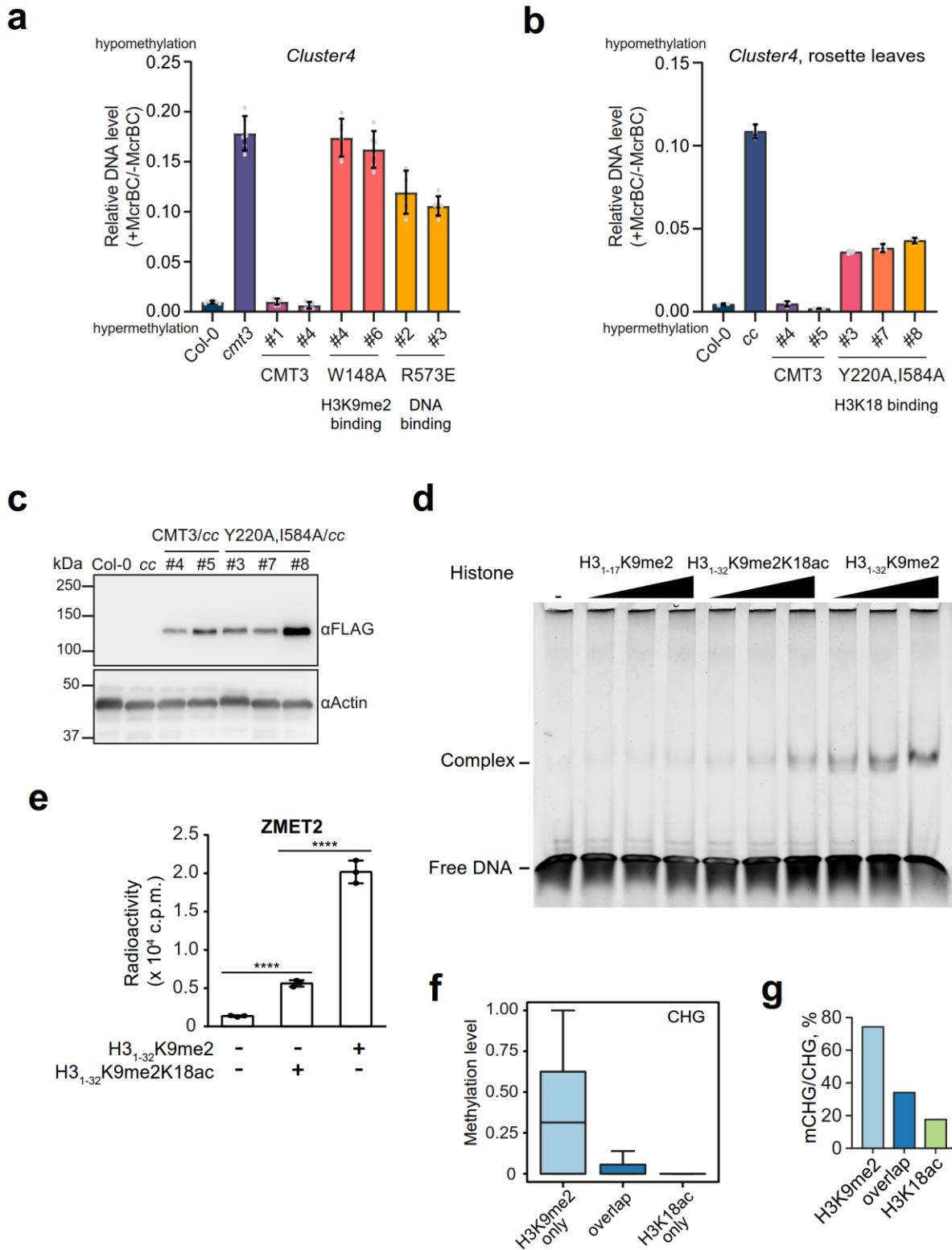
(a) Phenotypes of 3-week-old Arabidopsis expressing wild-type and mutant CMT3-FLAG in *cmt3* mutant background. Col-0 and *cmt3* served as controls. (b) Immunoblots showing the CMT3 protein level of the same lines in panel (a). Actin served as a loading control. (c) The relative transcript level of TE *Copia11* and gene *AT5G26970* was measured with reverse-transcription quantitative PCR in the transgenic lines. The RNA

transcript was normalized to *ACT7*. Data are mean \pm s.d. (n=6 technical replicates from n=2 independent experiments). (d) Phenotypes of 3-week-old Arabidopsis expressing wild-type and mutant CMT3-FLAG in *cmt2 cmt3* (*cc*) mutant background. (e) Immunoblots showing the CMT3 protein level of the same lines in panel (d). Actin served as a loading control. (f) DNA methylation of *Cluster4* locus in Arabidopsis transgenic lines in *cc* background measured by McrBC-qPCR assay. Data are mean \pm SD from three technical replicates. (g) The relative transcript level of TE *SADHU3-2* and gene *AT5G26270* in the transgenic lines in *cc* background. Data are mean \pm s.d. (n=6 technical replicates from n=2 independent experiments). Source data are provided as a Source Data file.



Supplementary Fig. 6 | Structural and biochemical analysis of the H3 peptide readout by CMTs

(a, b) Close-up view of the interaction between ZMET2 CD and H3₁₋₃₂K9me₂ peptide in the ZMET2-hmCAG-H3₁₋₃₂Kc9me₂ (a) or ZMET2-H3₁₋₁₅K9me₂ (4FT2) (b) complex. The hydrogen bonds are shown as dashed lines. Note that residues Q429-S434 of ZMET2 are disordered in the ZMET2-H3₁₋₁₅K9me₂ complex (PDB 4FT2), presumably due to the crystal packing effect. **(c,d)** Close-up view of the interaction between ZMET2 BAH and the N-terminal half (residues 1-12) of the H3₁₋₃₂Kc9me₂ peptide in the ZMET2-hmCAG-H3₁₋₃₂Kc9me₂ (c) or ZMET2-H3₁₋₃₂K9me₂ (4FT4) (d) complex. **(e)** Overlaid CD spectra of wild type (WT), Y302A, and M641A ZMET2 protein. **(f)** Thermal shift assay for the WT, Y302A, and M641A ZMET2 protein, with the raw fluorescence data shown. **(g)** DNA methylation rate of WT, Y302A, and M641A ZMET2 protein as a function of substrate concentration. Data points and the corresponding mean (bar) are derived from n=2 independent measurements. **(h)** The steady-state Michaelis–Menten parameters of WT, Y302A and M641A ZMET2 derived from (g). The mean and error estimate were derived from curve fitting. Source data are provided as a Source Data file.



Supplementary Fig. 7 | Functional analysis of the allosteric activation of CMT3/ZMET2 by the H3K9me2/H3K18 readout

(a) DNA methylation of *Cluster4* locus in *Arabidopsis* transgenic lines in *cmt3* background measured by McrBC-qPCR assay. 10-d-old seedlings were used. Data are mean \pm s.d. (n=6 technical replicates from n=2 independent experiments). (b) DNA methylation of *Cluster4* locus in *Arabidopsis* transgenic lines in *cc* background measured by McrBC-qPCR assay. The rosette leaves from 3-week-old plants were used. The Y220A,I584A/*cc* transgenic lines were in T₁ generation. Data are mean \pm s.d. (n=3 technical replicates). (c) Immunoblots showing the wild type and Y220A/I584A mutant CMT3 protein level in *cc* background. Actin served as a loading control. (d) EMSA analysis of the DNA-binding activity of ZMET2, in presence of different H3 peptides. The experiment was repeated twice with consistent results. (e) *In vitro* DNA methylation assays of ZMET2 on DNA containing single hmCHG site. Data are mean \pm s.d. (n = 3 biological replicates). Statistical analysis used two-tailed Student's t-test. ****, $p < 0.0001$. (f, g) CHG methylation level (f) and the ratio of methylated CHG over all CHG sites (mCHG/CHG) (g) of Col-0 in the peaks in Fig. 3j. The numbers of ChIP peaks are 1852 (H3K9me2 only), 206 (overlap), and 12036 (H3K18ac only). The lower and upper box edges correspond to the first and third quartiles, the horizontal lines indicate the median, and the lower and upper whiskers denote the smallest and largest values at most $1.5 \times$ IQR, respectively. Source data are provided as a Source Data file.

Supplementary Table 1. Data collection and refinement statistics.

	ZMET2-hmCAG-H3Kc9me2 (PDB: 7UBU)
Data collection	
Space group	P 2 ₁ 2 ₁ 2 ₁
Cell dimensions	
<i>a</i> , <i>b</i> , <i>c</i> (Å)	64.6, 121.4, 160.4
<i>a</i> , <i>b</i> , <i>g</i> (°)	90.00, 90.00, 90.00
Resolution (Å)	160.45-2.39(2.47-2.39) ^a
<i>R</i> _{merge}	0.129(1.873)
<i>I</i> / <i>s</i> (<i>I</i>)	10.1(0.8)
<i>CC</i> _{1/2}	0.992(0.380)
Completeness (%)	99.53(99.9)
Redundancy	5.7(6.0)
Refinement	
No. reflections	50,221
<i>R</i> _{work} / <i>R</i> _{free}	0.211/0.256
No. atoms	
Protein	5571
Peptide	240
DNA	733
SAH	26
Water	120
<i>B</i> factors (Å ²)	
Protein	74.0
Peptide	101.1
DNA	100.0
SAH	64.9
Water	68.0
r.m.s deviations	
Bond lengths (Å)	0.006
Bond angles (°)	0.855

^aValues in parentheses are for highest-resolution shell, which was determined based on *CC*_{1/2} > 0.3. Each structure was determined using the dataset collected from a single crystal.

Supplementary Table 2. Sequencing Statistics

Sample	Total reads	Aligned reads	% aligned	unique reads	% unique	*Fold Coverage	Bisulfite conversion
Col-0	59444216	56484853	95	44932612	75.6	18.9	99.6
<i>cmt3</i>	58331559	55602517	95.3	44187132	75.8	18.6	99.6
R745A/ <i>cmt3</i>	63566301	62199752	97.9	49485354	77.8	20.8	99.6
CMT3/ <i>cmt3</i>	52995070	51707665	97.6	41898929	79.1	17.60	99.5
H466A/ <i>cmt3</i> , 2	58822265	55626051	94.6	43660615	74.2	18.3	99.8
H466A/ <i>cmt3</i> , 4	41510535	36800534	88.7	29581372	71.3	12.4	99.8

*Fold coverage was calculated by multiplying the unique reads by the read length (50bp) and dividing it by the size of the Arabidopsis genome (119Mb).

Supplementary Table 3. List of primers used in this study

<i>Primers for Cloning and Site Directed Mutagenesis of CMT2/CMT3 in plants</i>			
Gene/TE	Gene/TE ID	Name	Primer Sequence (5'→3')
CMT3	AT1G69770	gCMT3-F	TTGTTCCGCGACATTGAATTCgatggtgatacagagacactact
CMT3	AT1G69770	gCMT3-R	CCAAGGGCGAATTGGTTCGACTGCAAGCTCGGAAGGAAGAG
CMT3	AT1G69770	W148A-F	CACGGCTCGGgcaTTTTATAGACCT
CMT3	AT1G69770	W148A-R	AGGTCTATAAAAtgcCCGAGCCGTG
CMT3	AT1G69770	H466A-F	TCAGTGGTgCcaACCGCTTC
CMT3	AT1G69770	H466A-R	GAAGCGGTTGgCcaCCACTGATT
CMT3	AT1G69770	R573E-F	GATCTAGTTCATgaAGGAAATATTGT
CMT3	AT1G69770	R573E-R	ACAATATTTCTtcATGAAGTAGATC
CMT3	AT1G69770	Y717A-F	cagGTTCCCGATgCtGCCTTAACAT
CMT3	AT1G69770	Y717A-R	ATGTTAAGGCAGcATCGGGAACctg
CMT3	AT1G69770	R745A-F	CTGTTGTCACAgcGGCAGAACCCC
CMT3	AT1G69770	R745A-R	GGGGTTCTGCCgCtGTGACAACAG
CMT3	AT1G69770	Y220A-F	CTATTTCTGCCTgCtCGATACATTTGAAG
CMT3	AT1G69770	Y220A-R	TTCAAATGTATCGgCtAGGCAAGAAATAG
CMT3	AT1G69770	I584A-F	atgcagGGAACgCtAGTAGCCTATGATG
CMT3	AT1G69770	I584A-R	CATCATAGGCTACTgCtGTTTCCctgcat
<i>Primers for qPCR</i>			
Cluster4	AT4G27930	Cluster4-F	CGTCCTCAAAGTTCCAGA
		Cluster4-R	GGTATTCTCCATCCCAAAG
Copia11	AT3G44215/	Copia11-F	TTGGAGACTAATCATACTTGGGAC

	AT3TE64435	Copia11-R	TAACCTTTGGCAACGAGACG
AT5G26970	AT5G26970	AT5G26970-F	TTGTCTCTATCCAAAGCCAC
		AT5G26970-R	GTCGGGAAAACTTTGGATTC
TM protein	AT5G26270	AT5G26270-F	CAAAATTTCTAGTGGTGCG
		AT5G26270-R	TTTCAAACGCCACCAAGAA
SADHU3-2	AT3G42658/ AT3TE60310	SADHU3-2-F	TTTTCTAGGTTTCGGTTCATAC
		SADHU3-2-R	TCCAATAGTACCAGCGATTACA
ACT7	AT5G09810	ACT7-F	CCTTCCAACAGATGTGGATTTTC
		ACT7-R	GTTCAATCCCATCTCAACTAGG
<i>Primers for Cloning and Site Directed Mutagenesis of CMT2, CMT3, ZMET2 and histone H3 tail for protein expression</i>			
CMT3	AT1G69770	CMT3_42F	A CAG ATT GGT GGATCC GAAGGGG AAAAGCATGT TG
CMT3	AT1G69770	CMT3_839R	C TTT ACC AGA CTCGAG TTATGCAAGCTCGGAAGGAA
H3		H3K9C_1WF	ACAGATTGGTGGATCCTGGGCCGTACCAAGCAGACCGCCCGTTGTCCA CCGGAG
H3		H3K9C_32R	CTTACCAGACTCGAGTTAGGTAGCAGGAGCGGACTTC
ZMET2		Y302A_F	CTCTGTTGCAGCTTCTACATTTGCTA
ZMET2		Y302A_R	AATGTAGAAGCTGCAACAGAGTAAGAC
ZMET2		F523A_F	TCAGTGGGGCTAATCGGTACAGAAAC
ZMET2		F523A_R	GTACCGATTAGCCCCACTGATACCTTGCCA
ZMET2		R630A_F	GTTGTAGTAGCTGGAGGAGCCCCTAATGC
ZMET2		R630A_R	CTCCTCCAGCTACTACAACATCATAGGTG
ZMET2		M641A_F	TCGCAATGTGCTGTTGCATATGACGAGAC
ZMET2		M641A_R	ATGCAACAGCACATTGCGAAAAGGCATTAG
ZMET2		D645AE646A_F	GGTTGCATATGCCGCTACACAAAAACCATCCCTG
ZMET2		D645AE646A_R	GTGTAGCGGCATATGCAACCATACATTGCG
ZMET2		Y776A_F	GGTTCCTGACGCTGCAATGTCATTATCAAG
ZMET2		Y776A_R	ACATTGCAGCGTCAGGAACAGTGGTTTCCC
ZMET2		R804A_F	AGTTGTAACCGCAGCAGAGCCTCACAACCAG
ZMET2		R804A_R	GCTCTGCTGCGGTTACAACTGTAGGAAGT
ZMET2		H808A_F	AGCAGAGCCTGCCAACCAGGTTATAATTCATCCG
ZMET2		H808A_R	CCTGGTTGGCAGGCTCTGCTCTGGTTACAAC
ZMET2		R630E_F	GTTGTAGTAGAAGGAGGAGCCCCTAATGCC
ZMET2		R630E_R	CTCCTCCTTCTACTACAACATCATAGGTGGGC
ZMET2		N635P_F	AGGAGCCCCTCCTGCCTTTTCGCAATGTATGG
ZMET2		N635P_R	GAAAAGGCAGGAGGGGCTCCTCCACGTACTAC
ZMET2		D645R_F	GGTTGCATATCGCGAGACAAAAACCATCCCTG
ZMET2		D645R_R	TTGTGTCTCGGATATGCAACCATACATTGCGAA
ZMET2		E646P_F	TGCATATGACCCTACACAAAAACCATCCCTGAAG
ZMET2		E646P_R	TTTTGTGTAGGGTCATATGCAACCATACATTGC

ZMET2		N524A_F	AGTGGGTTTGCTCGGTACAGAAACCGTGAT
ZMET2		N524A_R	TCTGTACCGAGCAAACCCACTGATACCTTG
ZMET2		R525A_F	GGGTTTAATGCGTACAGAAACCGTGATGAG
ZMET2		R525A_R	GTTTCTGTACGCATTAAACCCACTGATACC
ZMET2		Y526A_F	TTTAATCGGGCCAGAAACCGTGATGAGCC
ZMET2		Y526A_R	ACGGTTTCTGGCCCGATTAAACCCACTGATAC
CMT3	AT1G69770	Y220A_F	TTCTTGCCTGCGGATACATTTGAAGCTATACAAC
CMT3	AT1G69770	Y220A_R	AAATGTATCCGCAGGCAAGAAATAGTTCATGTC
CMT3	AT1G69770	I584A_F	CAGGGAAACGCAGTAGCCTATGATGAAGGAC
CMT3	AT1G69770	I584A_R	ATAGGCTACTGCGTTTCCCTGAAACTCCTTG